Rotating Magnetic Field Current Drive in FRCs

Alan L. Hoffman
University of Washington

A Rotating Magnetic Field (RMF) drives current by exerting a force on the electrons as shown in Fig. 1. Although $E_z \sim \sqrt{2}\omega\delta^* B_\omega$ at the edge increases with penetration depth δ^*, the force at the edge is relatively independent of the penetration depth δ^* since $j_z = -nev_{ez} = (\varpi/\omega)E_z/\eta_{//}$ decreases. In order for the RMF to penetrate, this force must exceed the resistive friction force so that the electron rotational speed ω_r becomes nearly synchronous. This condition is historicallly represented by requiring $\gamma > \lambda$. The RMF will then penetrate far enough to reverse the external field, at which point the FRC will expand radially against a flux conserver, increasing both the external field and current density until the forces (actually the total torques) are balanced (ie $\gamma \approx \lambda$). We experimentally use this condition as a measure of the effective cross field resistivity $\eta_\perp = m_e\nu_\perp/ne^2$.

$F_{\theta M} = ne\langle -v_{ez}B_r\rangle = \langle E_z^2\rangle\varpi/\omega^2 a\eta_{//}$ $\langle E_z\rangle \sim \omega\delta B_\omega$

$\delta = (2\eta_{//}/\mu_o\omega)^{1/2}$ $\omega_{ce} = eB_\omega/m_e$

$F_{\theta M} = 2B_\omega^2/\mu_o a$ $F_{\theta\eta} = (nm_e\omega_r a)\,\nu_\perp$

Call: l = **a**/d **g = w$_{ce}$/(n$_\wedge$n$_{//}$)$^{1/2}$**

If $\gamma > \lambda$ then $F_{\theta M} > F_{\theta\eta}$ and $\varpi = \omega - \omega_r << 1$

$\delta^* = (2\eta_{//}/\mu_o\varpi)^{1/2} > a$: RMF can penetrate

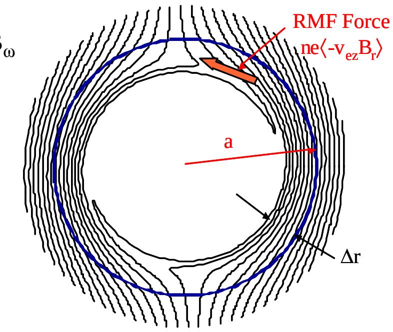

Figure 1. RMF force & resistive friction

As long as the electron density is high enough so that the maximum possible synchronous electron current $I'_{sync} = 0.5\langle n_e\rangle\omega a^2$ exceeds the necessary reversal current $I'_{rev} = B_e/2\mu_0$, the RMF can drive flux. We call the ratio of currents $\zeta = I'_{rev}/I'_{sync}$. If ζ is too low then current drive will be confined to a thin edge sheet, which will be both inefficient and incompatible with a normal FRC equilibrium. In equilibrium $E_\theta = 0$ everywhere and radial flow must drive current on the inner field lines. The RMF force must be sufficient to not only overcome the resistive friction on the outer field lines, but also reverse the normally outward diffusion. The values of v_r produced are shown on Fig. 2 in analytic form and from a 1-D MHD

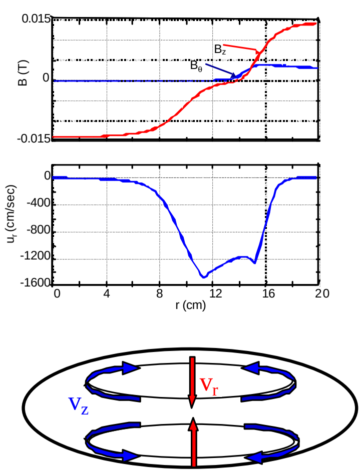

Generalized Ohm's Law

$$E_\theta = \eta_\perp j_\theta + v_r B_z + \langle j_z B_r\rangle/ne$$

In equilibrium ($E_\theta = 0$) $j_\theta = -|j_\theta|$

$$B_z > 0:\quad v_r = [\eta_\perp |j_\theta| - \langle v_{ez}B_r\rangle]/B_z$$

$$B_z < 0:\quad v_r = -\eta_\perp |j_\theta|/|B_z| = -(\eta_\perp/B_z^2)dp/dr$$

Radial Force Balance

$$\frac{dp}{dr} = j_q B_z + \langle -j_z B_q\rangle = \nabla\left\{\frac{B_z^2}{2m_o} + \frac{B_q^2}{4m_o}\right\}$$

Figure 2. Assumed flux sustainment methodology.

calculation. Since the total inward flow will create a higher pressure on the inner field lines, there must be flow along flux surfaces as also sketched on Fig. 2. This is the basic methodology we assume for the RMF drive process.

In initial experiments conducted on the smaller STX device the FRCs were long (~2 m) and skinny (r_s ~ 0.2 m). Flux could be built up, but not sustained for long periods. We assume that was due to density piling up on the inner field lines and not being able to flow around the FRC quickly enough to set up the flow pattern shown on Fig. 2. When this happened the absorbed RMF power sharply decreased and a high beta mirror configuration was formed. This was not the case for the larger TCS device, where the typical plasma lengths varied between 1.5 and 2.5 m, while the separatrix radius was slightly under the 0.4 m quartz plasma tube radius.

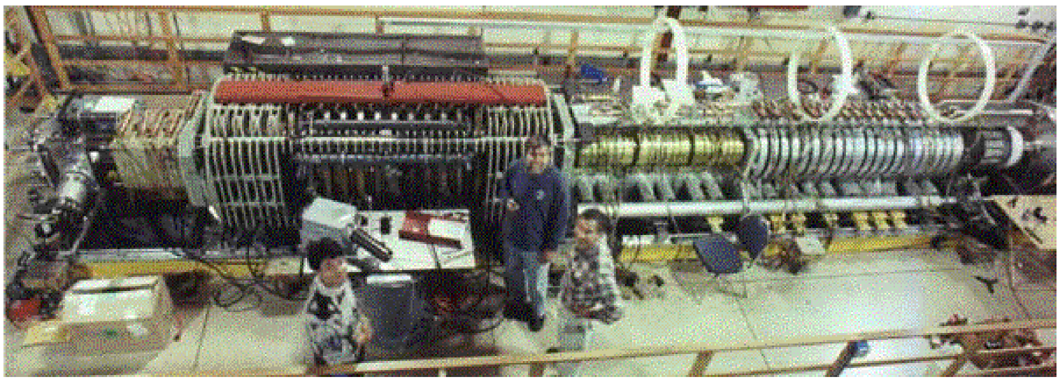

TCS Chamber
(confinement & RMF drive)

LSX/mod
(formation & 'acceleration')

Figure 3. The TSC facility

A picture of TCS is showen on Fig. 3. The facility was designed to form FRCs in the 2-m long by 40-cm diameter formation section, and be translated through a 27-cm diameter plasma tube (previously used for acceleration experiments) into the 2.5-m long by 80-cm diameter TCS section. RMF can be applied through 1.5-m long antenna loops (black wrapped 3" tubes in photograph) and a multi-MW power supply built by Los Alamos National Laboratory. Some initial translation and expansion experiments were conducted, but no RMF has yet been applied to these FRCs due to a nead to reduce impurities picked up upon reflection off the far stainless steel (with magnetic mirror) end cone.

Measurements of the flux time histories, as well as other parameters in TCS, are shown on Fig. 4 for three different puff-fill pressures. Below 4-mTorr fill pressures it became difficult to trap much flux in the formation section. One unexplained phenomenon, which has also been seen in the FIX experiments, is a much smaller FRC radius on the first pass than would be calculted from the flux measured after the first bounce. (This makes the inferred flux, $\phi_p = 0.97 x_s r_s^2 B_e$, also appear lower on the first pass.) After the first bounce the FRCs display flux levels comensurate with those measured in the formation section, and then decay with about 200 μsec lifetimes. For the lower density FRCs, this implies resistivities ($D_\perp = \eta_\perp/\mu_o$) about a factor of two less than the previous high LSX based empirical scaling. The same results have been seen in the FIX experiments.

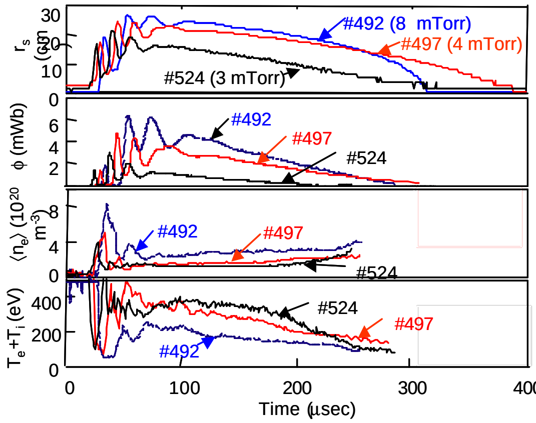

B_o = 1 kG

n_{20} = 1-3 ($10^{20}m^{-3}$)

$\tau_\phi = r_s^2/16D_\perp \approx 200$ μsec

$\Rightarrow D_\perp \approx 10\ m^2/sec$

$\{D_{\perp empirical} \approx 19/(n_{20})^{1/2}\}$

Figure 4. Non-sustained FRCs in TCS

TCS was used to form FRCs from a preionized gas puff. Results are shown on Fig. 5 for initial operation at a 170 kHz RMF frequency. In order to achieve this steady-state type operation it was necessary to allow the FRC to extend beyond the ends of the RMF antenna, perhaps related to the ability to sustain the 3-D flow pattern shown on Fig. 2. The listed resistivity was calculated by assuming that the FRC reached final conditions given by $\gamma/\lambda = 1/\sqrt{2}$ based on the following analytical formulas.

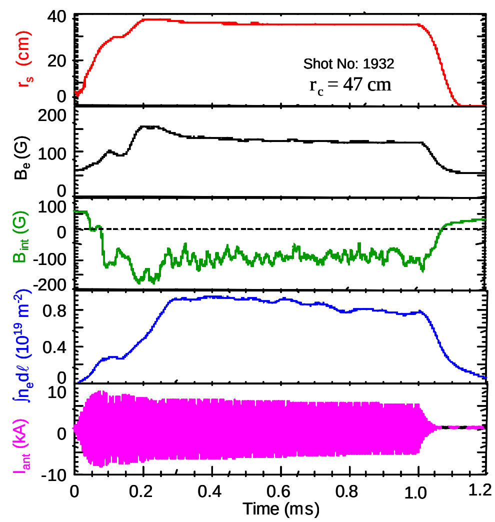

ω = 1060 kHz

B_o = 60 G

B_ω = 40 G

<u>At t = 400 μsec</u>

$\langle n_e\rangle = 0.7\times10^{19}\ m^{-3}$

$\eta_\perp(\gamma/\lambda=1/\sqrt{2}) = 180\ \mu\Omega\text{-m}$

$\tau_\phi = r_s^2/16(\eta_\perp/\mu_o) = 52$ μsec

$\zeta = 0.31$

$\eta_{\perp empirical} = 60\ \mu\Omega\text{-m}$

Figure 5. FRC generation from preionized gas puff.

$$\frac{d f}{dt} = \frac{2}{ner_s^2}\left(T_M - T_h\right) \qquad T_o = \frac{2pr_s^2 B_w^2}{m_o}$$

$$T_M \approx 0.3\zeta T_o \qquad [1]$$

$$T_\eta \approx \pi\omega r_s^4 n_m^2 e^2 \eta_\perp (0.15\,\zeta) = \frac{l^2}{2g^2}[0.3\zeta T_o]$$

In these formulas γ is based on the peak density n_m so that $\nu_\perp = n_m e^2\eta_\perp/m_e$. The resistivity calculated in this manner is high, but is probably overestimated since the FRC is only driven over about 60% of its length and, for the low value of ζ, a value of γ/λ

closer to unity is required. However, the resistivity still appears higher than the old empirical scaling. We think this is due to the low ion temperatures (only a few eV) and very high ratios of electron drift speed to ion sound speed. Hopefully this will be resolved when we apply RMF to the hot translated FRCs.

Experiments were also conducted at a 70 kHz RMF frequency to try and increase ζ, and thus the depth of the necessary current layer. However, this primarily resulted in an increase in density, with only a slight increase in ζ. In retrospect, this can be seen from the formula

$$\frac{g}{l} = \frac{0.007B_w(\mathrm{G})}{n_\mathrm{m}(10^{20}\mathrm{m}^{-3})D_\perp^{1/2}(\mathrm{m}^2/s)w^{1/2}(\mathrm{MHz})r_s(\mathrm{m})} \, . \qquad [2]$$

For a given value of resistivity (represented by $D_\perp = \eta_\perp/\mu_o$) the density will just increase until Eq. (2) is satisfied. It would be possible to produce higher external fields if the temperature increased, but in our present experiments the temperature appears limited to about 50 eV by a high neutral background and large radiation losses.

Table 1
Optimal extension of TCS Results

Parameter	TCS	TCS_{trans}	Reactor
r_s (m)	0.35	0.35	3.50
B_e (T)	0.02	0.10	1.0
n_m (10^{20} m^{-3})	0.25	1.0	1.0
T_e (keV)	0.05^	0.125*	12.5*
ω (10^6 s^{-1})	0.5	0.3	0.03
B_ω(G) required for $\gamma/\lambda = 1/\sqrt{2}$ (B_ω available or planned)	$6.3D_\perp^{1/2}$ 60	$20D_\perp^{1/2}$ (75)	$65D_\perp^{1/2}$ (50 -100)*
P_{abs} (MW/m)	$0.016\eta_\perp$	$0.2\eta_\perp$	$20\eta_\perp$
ϕ (Wb)	0.002	0.01	10
s		3	30

It is interesting to look at where we are now, where we would like to go in the near future, and what would be required for a reactor sustained by RMF alone. For the present first column TCS results the total pressure balance temperature was 50 eV, which we assume was mostly in the electrons. For the other two cases we stipulate $T_e = T_i$. It is seen that the present FRCs can be driven with resistivity values as high as 100 μΩ-m (the units of $\eta_\perp$ in table 1). For the translated experiments to be successful, the resistivity must be reduced to under 15 μΩ-m, which is consistent with the empirical scaling for hot-ion FRCs. For a reactor sustained by RMF alone the resistivity must be reduced by another order of magnitude. This can be seen from the absorbed power row, since such a plasma would produce about 150 MW/m of fusion power.

At the lower 70 kHz RMF frequencies in TCS the FRCs were observed to spin up to about 10% of the RMF frequency and sometimes result in an n=2 instability if the FRCs were short and not close to the wall. We attribute this lack of full spin up to the RMF frequency to be due to collisions with neutrals. Some other measure, such as tangentially injected neutral beams, will most likely be required for long time experiments at higher densities where the neutral fraction will be lower. An FRC driven by both RMF and tangential NB appears to be the ideal solution. If a strong NB source was available to produce hot-ion plasmas, the RMF could be used to reverse the field and form an FRC. This would eliminate the need to start with a theta-pinch formed hot-ion FRC, and considerably simplify experimental design.